Cell

Article

Muscle Spindle Feedback Directs Locomotor Recovery and Circuit Reorganization after Spinal Cord Injury

Aya Takeoka,[1,2,4] Isabel Vollenweider,[3,4] Grégoire Courtine,[3,5] and Silvia Arber[1,2,5,*]
[1]Biozentrum, Department of Cell Biology, University of Basel, 4056 Basel, Switzerland
[2]Friedrich Miescher Institute for Biomedical Research, 4058 Basel, Switzerland
[3]Brain Mind Institute and Centre for Neuroprosthetics, Ecole Polytechnique Fédérale de Lausanne (EPFL), 1015 Lausanne, Switzerland
[4]Co-first author
[5]Co-senior author
*Correspondence: silvia.arber@unibas.ch
http://dx.doi.org/10.1016/j.cell.2014.11.019

SUMMARY

Spinal cord injuries alter motor function by disconnecting neural circuits above and below the lesion, rendering sensory inputs a primary source of direct external drive to neuronal networks caudal to the injury. Here, we studied mice lacking functional muscle spindle feedback to determine the role of this sensory channel in gait control and locomotor recovery after spinal cord injury. High-resolution kinematic analysis of intact mutant mice revealed proficient execution in basic locomotor tasks but poor performance in a precision task. After injury, wild-type mice spontaneously recovered basic locomotor function, whereas mice with deficient muscle spindle feedback failed to regain control over the hindlimb on the lesioned side. Virus-mediated tracing demonstrated that mutant mice exhibit defective rearrangements of descending circuits projecting to deprived spinal segments during recovery. Our findings reveal an essential role for muscle spindle feedback in directing basic locomotor recovery and facilitating circuit reorganization after spinal cord injury.

INTRODUCTION

Spinal cord injury has an immediate and devastating impact on the control of movement. The origin of motor impairments lies in the physical disconnection of descending pathways from spinal circuits below the lesion, depriving them of synaptic input essential for the generation and regulation of motor output. Despite the failure of severed axons to regenerate at long distance (Ramon y Cajal, 1928; Tello, 1907), partial lesions of the human spinal cord are frequently associated with spontaneous functional improvement (Curt et al., 2008). One of many challenges in restoring motor control after spinal cord injury is to re-establish a sufficient level of task-specific excitability within disconnected local spinal circuits to drive motor neurons caudal to the injury.

Recent studies on incomplete spinal cord injury animal models uncovered some of the mechanisms that may contribute to spontaneous motor recovery (Ballermann and Fouad, 2006; Bareyre et al., 2004; Courtine et al., 2008; Jankowska and Edgley, 2006; Rosenzweig et al., 2010; Zörner et al., 2014). These investigations showed that recovery correlates with the establishment of intraspinal detour circuits. Such alternative pathways through the spared tissue form novel functional bridges across the lesioned spinal segments. At present, circuit-level mechanisms promoting the formation of detour circuits to restore control of movement remain elusive, even though such insight might play a pivotal role in developing interventions that enhance locomotor recovery after spinal cord injury.

Various studies suggest that sensory information plays a critical role in gait control and in locomotor recovery after spinal cord injury (Edgerton et al., 2008; Pearson, 2008; Rossignol et al., 2006; Rossignol and Frigon, 2011; Windhorst, 2007). The most common medical practice used to facilitate motor recovery of paraplegic patients is weight-supported locomotor rehabilitation (Dietz and Fouad, 2014; Knikou and Mummidisetty, 2014; Roy et al., 2012). Repetitive movement during rehabilitative training likely enhances glutamatergic dorsal root ganglia (DRG) sensory feedback, which constitutes the primary extrinsic source of excitation entering the spinal cord below injury to engage local spinal circuits. This interpretation is supported by evidence from animal models in which spinal cord injury coupled to partial or complete elimination of sensory input impairs gait control and locomotor recovery (Bouyer and Rossignol, 2003; Lavrov et al., 2008). However, the DRG neuron subtype promoting locomotor recovery and the mechanisms by which this process takes place are unclear.

Proprioceptive sensory neurons innervate sense organs in the muscle and transmit information about muscle contraction to the spinal cord (Brown, 1981; Rossignol et al., 2006; Windhorst, 2007). Their influence on the activity of central circuits is essential for modulation and adjustment of motor output (Pearson, 2008; Rossignol et al., 2006). Muscle spindle afferents constitute a subset of proprioceptors contacting muscle spindle sense organs. They exhibit the most widespread central projection pattern of all DRG sensory neurons and establish

synaptic contacts with motor neurons and various classes of interneurons implicated in motor control (Brown, 1981; Eccles et al., 1957; Rossignol et al., 2006; Windhorst, 2007). Muscle spindle afferents are thus in a prime position to convey direct excitation to spinal circuits relevant to the regulation of motor behavior, especially under conditions of disconnected descending input.

The zinc-finger transcription factor Egr3 is expressed selectively by muscle spindle-intrinsic intrafusal muscle fibers, and its mutation results in early postnatal degeneration of muscle spindles (Tourtellotte and Milbrandt, 1998). This defect abolishes normal function of muscle spindle afferents as assessed electrophysiologically (Chen et al., 2002) and leads to gait ataxia (Tourtellotte and Milbrandt, 1998). *Egr3* mutant mice thus represent a genetic model with DRG sensory neuron dysfunction selectively restricted to muscle spindle afferents. They provide an opportunity to investigate how this feedback channel contributes to gait control in intact mice and influences locomotor recovery and circuit reorganization after spinal cord injury.

To address this question, we conducted kinematic analyses in wild-type and *Egr3* mutant mice. Deficiency of muscle spindle feedback did not affect basic motor abilities in intact *Egr3* mutant mice beyond specific gait features. However, lack of muscle spindle feedback severely restricted spontaneous recovery after incomplete spinal cord injury. *Egr3* mutant mice also exhibit a markedly reduced ability to establish descending detour circuits restoring access to spinal circuits below spinal cord injury. We conclude that muscle spindle feedback is a key neuronal substrate to direct circuit rearrangement necessary for locomotor recovery after incomplete spinal cord injury.

RESULTS

Proficient Basic Locomotion in Absence of Muscle Spindle Feedback

We performed high-resolution video recordings to reconstruct hindlimb kinematics in wild-type and *Egr3* mutant mice (Figures 1A and 1B). We focused on task-dependent contributions of muscle spindle input to hindlimb motor control with the aim to establish a baseline to which we could compare the locomotor recovery process after spinal cord injury.

We first assessed hindlimb motor control during basic overground locomotion. Wild-type and *Egr3* mutant mice performed this task with reciprocal activation of flexor and extensor muscles and alternation between left and right hindlimbs (Figure 1B; Movie S1 available online). However, *Egr3* mutant mice exhibited gait ataxia as reported previously (Tourtellotte and Milbrandt, 1998). To characterize gait patterns, we computed >100 kinematic parameters that provide a comprehensive quantification of locomotor features (Figure S1) (Courtine et al., 2008). We subjected all measured parameters to a principal component (PC) analysis (van den Brand et al., 2012) (averaged values of 10–25 step cycles/hindlimb/mouse; n = 22 wild-type and n = 19 *Egr3* mutants; Figure S2). We then visualized gait patterns in the new space created by PC1–3, where PC1 explained the highest variance (18%) and distinguished the two genotypes (Figure 1C). The locomotor phenotype observed in *Egr3* mutant mice was limited to distinct gait features represented in PC1 and approximately 65% of all parameters did not correlate with this genotype-specific PC1 (Figure S3A).

To evaluate the ability of *Egr3* mutant mice to adjust gait patterns to changing locomotor velocities, we tested mice during stepping on a treadmill. Both wild-type and *Egr3* mutant mice were capable of stepping across the entire range of tested treadmill speeds (7–23 cm/s; Figures 1D and S3B). PC1 captured adjustment of gait patterns with increasing speed in mice of both genotypes (16% of explained variance; Figures 1D and S3C), whereas PC2 segregated genotypic differences independent of velocity (10% explained variance; Figures 1D and S3C). Electromyogram (EMG) recordings of ankle extensor and flexor muscles revealed that both genotypes showed appropriate speed-dependent adjustments in burst duration (Figure 1D). These findings resonate with work demonstrating that the flexion phase of the step cycle remains constant, whereas the extension phase progressively shortens with increased locomotor speed (Arshavskiĭ et al., 1965; Halbertsma, 1983), a property we now demonstrate to be independent of muscle spindle sensory feedback.

In summary, both wild-type and *Egr3* mutant mice are able to perform basic locomotor tasks proficiently, but mutant mice display specific gait alterations concordant with the previously proposed role of muscle spindle feedback in control and adjustment of locomotion (Pearson, 2008; Rossignol et al., 2006; Windhorst, 2007).

Muscle Spindle Feedback Is Essential for Locomotor Precision Task and Swimming

Next, we tested mice of both genotypes during walking on a horizontal ladder, requiring precision in foot placement. Whereas wild-type mice progressed across the ladder with ease, *Egr3* mutants frequently slipped off or missed rungs, which was reflected in aberrant bouts of EMG activity (Figure 2A; Movie S2). Quantification of foot positioning relative to successive rungs revealed that wild-type mice targeted rungs precisely, whereas *Egr3* mutant mice displayed near-random foot placement (Figure 2B). These findings demonstrate an essential role for muscle spindle feedback circuits in the regulation of accurate foot placement in a locomotor precision task.

Egr3 mutant mice exhibit selective defects of muscle spindle feedback, but other sensory feedback is preserved (Tourtellotte and Milbrandt, 1998). During swimming, afferents from Golgi tendon organs are attenuated due to reduced weight load (Gruner and Altman, 1980). Proprioceptive signaling therefore relies almost exclusively on muscle spindle feedback. We found that during swimming, wild-type mice displayed well-coordinated alternation of left and right hindlimbs with reciprocal activity of ankle flexor and extensor muscles (Figures 2C and 2D). In contrast, *Egr3* mutant mice were unable to keep afloat and showed uncoordinated hindlimb movements with extensive coactivation of antagonistic muscles (Figures 2C and 2D). Together, these findings stress the pivotal function of muscle spindle feedback in the control of swimming, a condition when Golgi tendon organ and cutaneous feedback circuits only play a limited task-related function.

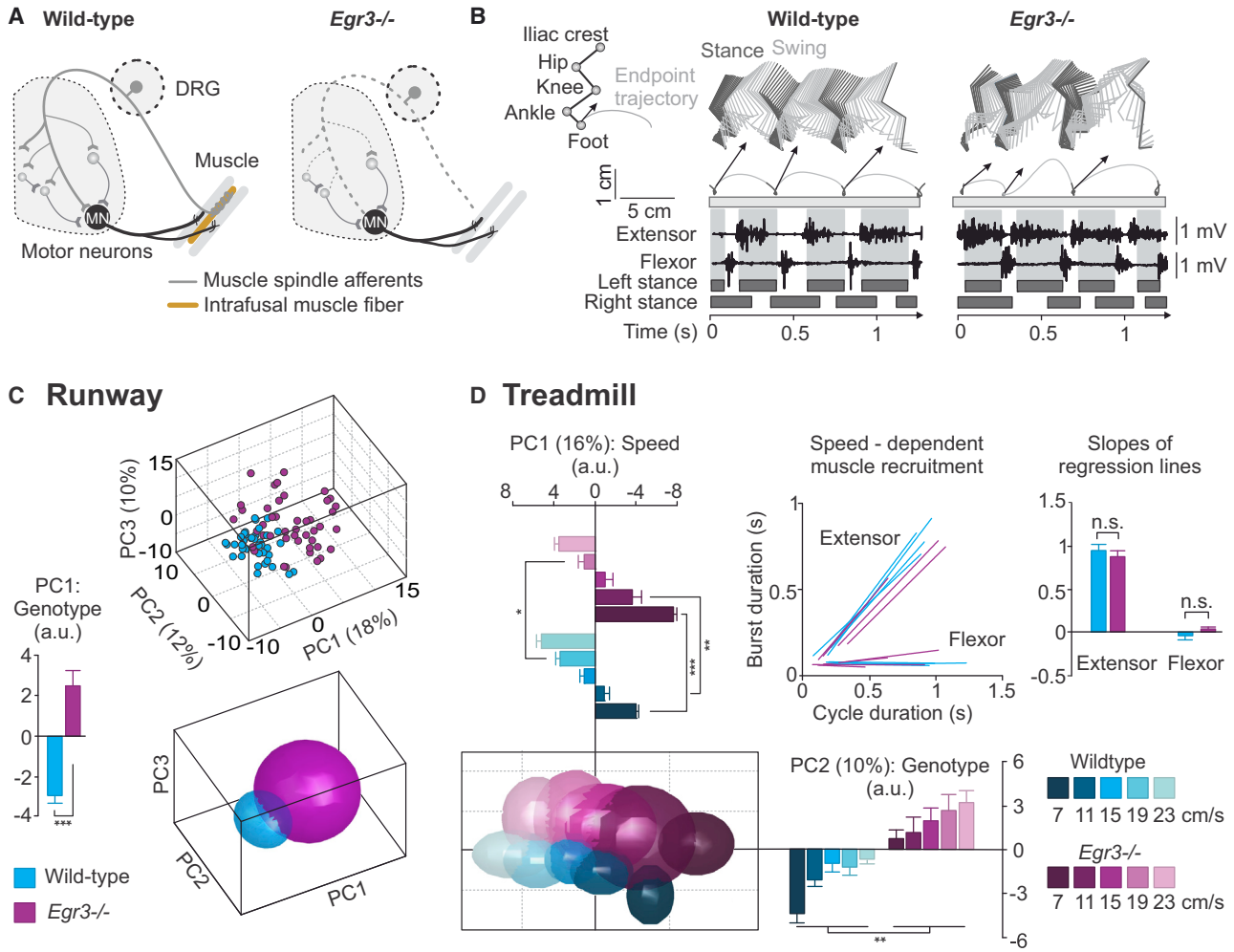

Figure 1. Proficient Basic Locomotion in Absence of Muscle Spindle Feedback

(A) *Egr3* mutation results in selective degeneration of muscle spindles and nonfunctional muscle spindle feedback circuits.

(B) Color-coded stick decomposition of hindlimb movement during three consecutive steps with limb endpoint trajectories and velocity vector at swing onset during basic overground locomotion in both genotypes (EMG activity of an extensor and a flexor muscle displayed below; dark gray bars, stance; empty spaces, swing).

(C) PC analysis was applied on 103 gait parameters measured during overground locomotion (10–25 gait cycles/hindlimb/mouse, n = 22 wild-type and n = 19 *Egr3* mutants). Gait cycles are represented for each animal and hindlimb (individual dots) in the new space created by PC1–3. Least-squares elliptical fitting (95% confidence) was computed to emphasize differences between genotypes. Histogram plot, mean values of PC1 scores for each genotype.

(D) PC analysis applied on averaged values of 108 gait parameters (15–30 gait cycles/mouse/speed, n = 10 for each genotype) measured during stepping on a treadmill at five different speeds (7–23 cm/s). Histogram plots, mean values of PC1 and PC2 scores. Correlation between step-cycle duration and extensor or flexor burst duration. Each regression line was computed separately for a given animal (n = 4 for each genotype; 25–30 step cycles/mouse). Histogram plots, slopes of regression lines for extensor and flexor muscles.

*p < 0.05; **p < 0.01; ***p < 0.001; ns, not significant; error bars, SEM; extensor, gastrocnemius medialis; flexor, tibialis anterior; a.u., arbitrary unit. See also Figures S1, S2, and S3 and Movie S1.

Muscle Spindle Feedback Circuits Are Essential for Locomotor Recovery after Injury

The core ability to perform basic locomotion is not disturbed in *Egr3* mutant mice, providing an opportunity to assess the role of muscle spindle feedback circuits in gait control and spontaneous recovery after spinal cord injury. We placed a lateral hemisection injury at the thoracic level (T10) and confirmed lesion completeness upon termination of experiments (Figure 3A). This lesion interrupts descending tracts projecting ipsilateral to lesion (ipsilesional hereafter), which normally innervate lumbar segments containing circuits essential for the control of ipsilesional hindlimb muscles (Figure 3A). We performed kinematic analysis at regular intervals after injury to follow locomotor recovery (Figures 3A and 3B).

Three days after injury (acute), both wild-type and *Egr3* mutant mice dragged the ipsilesional hindlimb along the runway as they moved forward (Figure 3B; Movies S3 and S4). Wild-type mice gradually regained locomotor proficiency over the time course

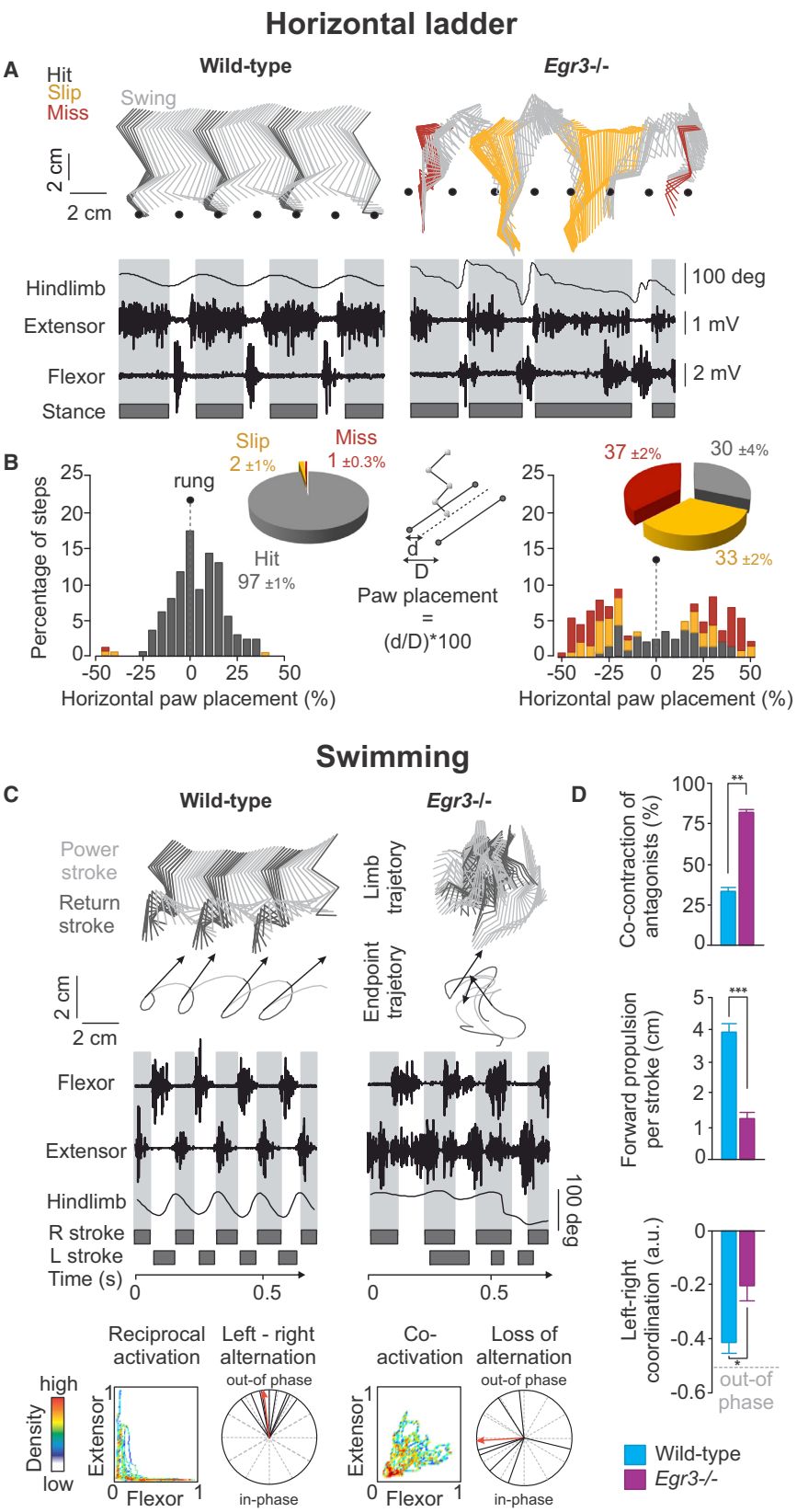

Figure 2. Muscle Spindle Feedback Is Essential for Precision Tasks and Swimming

(A) Stick diagram decomposition of hindlimb movement for a representative wild-type and *Egr3* mutant mouse during crossing of an elevated horizontal ladder with rungs (spacing 2 cm; below: hindlimb oscillation and traces of ankle extensor and flexor muscles for same mouse; dark gray bars, stance).

(B) Bar graph quantifying relative positioning of hindpaws with respect to rung positions. Pie charts summarize total percentage of hits, slips, and misses (n = 9 mice per genotype; 259 steps for wild-type and 323 steps for *Egr3* mutant mice).

(C) Stick decomposition of hindlimb movement for a wild-type and *Egr3* mutant mouse during swimming (below: limb endpoint trajectories, limb endpoint velocity vectors at power stroke onset, and raw traces of muscle activity for an extensor and flexor muscle together with hindlimb oscillations; dark gray bars, return stroke). Density plot displays coordination between antagonistic muscles during the represented trial (L-shaped patterns, reciprocal muscle activation; diagonal: continuous coactivation). Polar plot, coordination between left and right hindlimb oscillations (black lines, single gait cycle; red arrow, average of all gait cycles).

(D) Histogram plots report mean values for representative kinematic and muscle activity-related variables extracted from PC analysis (n = 181 swim strokes, 10–15 strokes/mouse, n = 8 wild-type and n = 7 *Egr3* mutant mice) during swimming task.

*p < 0.05; **p < 0.01; ***p < 0.001; error bars, SEM; extensor, vastus lateralis; flexor, tibialis anterior; a.u., arbitrary unit. See also Figures S1 and S2 and Movie S2.

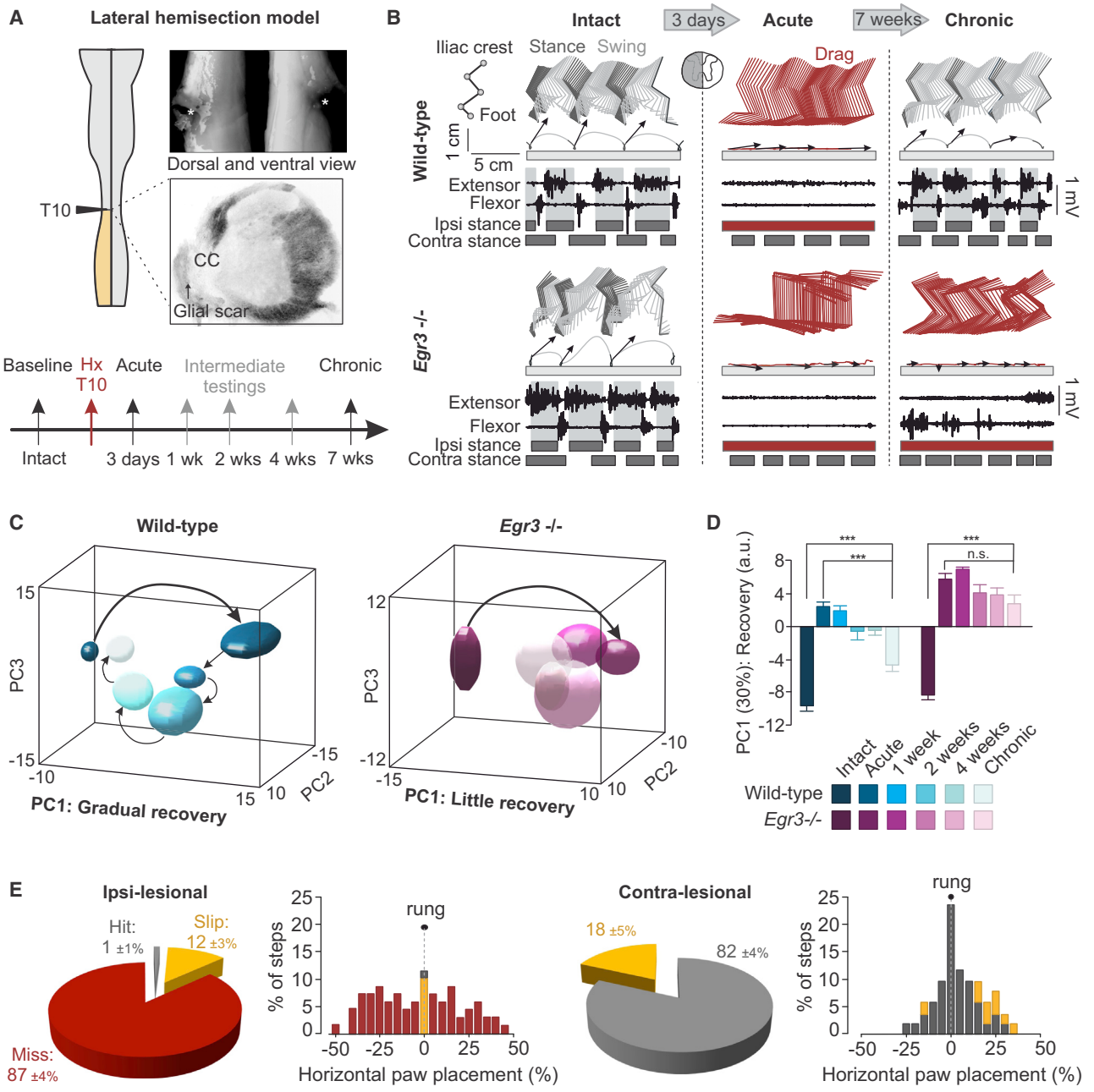

Figure 3. Muscle Spindle Feedback Is Essential to Direct Spontaneous Locomotor Recovery after Lateral Hemisection

(A) Illustration of thoracic lateral hemisection model, including a representative lesion from a dorsal, ventral, and coronal view, and time line of experiment procedures.

(B) For each genotype, a representative stick decomposition of hindlimb movement during basic overground locomotion is shown for intact, acute, and chronic time points for the same mouse (below: concurrent limb endpoint trajectory and velocity vector at swing onset, activity of an extensor muscle, and activity of a flexor muscle; dark gray bars, stance; red bars, dragging).

(C) Representation of gait clusters in PC space for one mouse per genotype during intact stepping and at five different time points postinjury (10–15 steps per time point; 103 parameters per gait cycle).

(D) Histogram plots reporting mean values of PC1 scores measured on all data combined (average of 10–25 steps per time point, 103 parameters per gait cycle, n = 9 wild-type mice, n = 7 *Egr3* mutant mice).

(E) Bar graph of relative positioning of hindpaws with respect to rung positions for chronically injured wild-type mice (n = 10). Pie charts summarize total percentage of hits, slips, and misses (n = 259 steps contralesional hindlimb; n = 147 steps ipsilesional hindlimb).

*p < 0.05; ***p < 0.001; ns, not significant; error bars, SEM; extensor, medial gastrocnemius; flexor, tibialis anterior; Hx, hemisection; a.u., arbitrary unit; acute, 3 days postinjury; chronic, 7 weeks postinjury. See also Figures S1, S2, and S4 and Movies S3, S4, and S5.

analyzed. By 7 weeks postinjury (chronic), they regained weight-bearing plantar steps with regular alternation of stance and swing phases of the ipsilesional hindlimb (Figures 3B and S4A; Movies S3 and S4). In contrast, *Egr3* mutant mice still exhibited severe locomotor deficits at the chronic stage (Figures 3B and S4A; Movies S3 and S4).

To quantitatively assess the recovery of ipsilesional hindlimb function, we conducted a PC analysis comparing intact condition to each time point evaluated. We found that PC1 characterized the recovery process (30% explained variance; Figures 3C and 3D). In wild-type mice, time-dependent gait clusters gradually moved toward intact conditions, reflecting the progressive recovery of locomotor function (Figures 3C and 3D). In contrast, gait clusters of *Egr3* mutant mice remained confined in the same PC space through the entire time course evaluated (Figures 3C and 3D). Detailed kinematic analysis revealed that in chronic wild-type mice, 73% of all parameters affected at acute stages improved significantly ($p < 0.05$) and 17% even recovered to levels measured before lesion (Figure S4A). Lack of locomotor recovery in *Egr3* mutant mice was associated with persistent dragging of the ipsilesional hindlimb at all time points (Figures 3B and S4A). In addition, analysis of contralesional hindlimb gait parameters revealed that both wild-type and *Egr3* mutant mice adjust their gait to ipsilesional hindlimb deficiencies similarly and immediately after lesion (Figure S4B). Together, our results demonstrate that defective muscle spindle feedback circuitry severely limits spontaneous locomotor recovery after incomplete spinal cord injury.

Speed Adjustment, but Not Precision Control, Improves in Wild-Type Mice after Injury

Next, we determined the extent to which hemisected wild-type mice regain the capacity to accommodate hindlimb movement to increasing walking speeds and to perform muscle spindle feedback-dependent swimming and ladder precision tasks.

Wild-type mice at chronic stages recovered the ability to walk at the highest speed tested (23 cm/s). After a lack of ipsilesional muscle recruitment at acute stages, the modulation of ankle extensor muscle activity gradually recovered toward intact levels (Figure S4C). In contrast, prolonged paw dragging (Figure S4A) led to increased EMG bursts in ankle flexor muscles after lesion, a feature that only partially recovered at chronic stages (Figure S4C). Wild-type mice regained well-coordinated limb alternation during swimming (Figure S4D) (Zörner et al., 2010), providing further evidence for recovery of basic locomotor features. During precision walking on the horizontal ladder at chronic stages, 87% of ipsilesional hindlimb steps resulted in a complete miss of the targeted rung, and 12% slipped off the rung. In contrast, most steps of the contralesional hindlimb were placed correctly on the rungs (82%) (Figure 3E; Movies S5).

Taken together, these results indicate that after lateral hemisection injury, wild-type mice regain basic locomotor function but only partially recover speed-dependent adaptation and completely fail to recover precise paw placement required for ladder locomotion.

Muscle Spindle-Specific Feedback Needed for Functional Recovery

Contrary to wild-type mice that regained the ability to move their ipsilesional hindlimb after injury, *Egr3* mutants exhibited persistent lack of locomotor control. Because activity-dependent mechanisms contribute to recovery of locomotor function after spinal cord injury (Dietz and Fouad, 2014; Edgerton et al., 2008; Maier and Schwab, 2006), we next measured the degree of spontaneous motility in *Egr3* mutant mice. We monitored home cage activity before injury and at regular intervals after lesion (Figure 4A). Both groups displayed decreased locomotor activity immediately after injury, but there were no significant genotype-related differences in distance covered throughout the recovery process (Figure 4A).

We then asked whether daily administration of monoaminergic receptor agonists known to acutely enhance locomotor output in rodents with severe spinal cord injury (van den Brand et al., 2012) influence the recovery process in *Egr3* mutant mice. We reasoned that despite indistinguishable motility between the two groups after lesion, spinal circuits in *Egr3* mutants may be recruited less efficiently in the absence of functional muscle spindle feedback than in wild-type mice. We found that upon daily agonist administration, *Egr3* mutants still exhibited an overall impediment in locomotor recovery (Figures 4B and 4C). The contribution of individual parameters to the recovery-associated PC1 showed a high correlation between spontaneous and daily drug administered groups for both genotypes (Figure 4D). These results demonstrate that muscle spindle sensory feedback is absolutely essential for directing the process of locomotor recovery after spinal cord injury and cannot be substituted for by daily activation of spinal circuits through pharmacological means.

Muscle Spindle Feedback Promotes Efficient Detour Circuit Establishment around Lesion

Because reorganization of supraspinal and intraspinal descending circuits parallels spontaneous recovery after incomplete spinal cord injury (Bareyre et al., 2004; Courtine et al., 2008; Rosenzweig et al., 2010; Zörner et al., 2014), we asked whether presence of muscle spindle feedback influences these injury-induced circuit reorganization responses. The formation of functional detour circuits relies on the ability of neuronal subpopulations to establish new connections to ipsilesional spinal circuits below the lesion. A predicted hallmark of such neurons is that they must have projections to segments below injury prior to lesion and establish novel synaptic connections after injury.

To identify sources of such neurons, we performed a mapping approach to label neurons with projections to the ipsilesional lumbar spinal cord, by injection of G protein-deficient rabies viruses encoding fluorescent marker proteins (FP) (Rab-FP; Figure 5A) (Wickersham et al., 2007). We analyzed the relative abundance and pattern of marked neurons above lesion in intact, acute, and chronic mice.

We first visualized descending supraspinal projection neurons in intact wild-type and *Egr3* mutant mice. Retrogradely labeled neuron distribution was reminiscent of patterns of mapped premotor brainstem nuclei (Esposito et al., 2014), with most Rab-FP^{ON} neurons located in the magnocellular, followed by pontine,

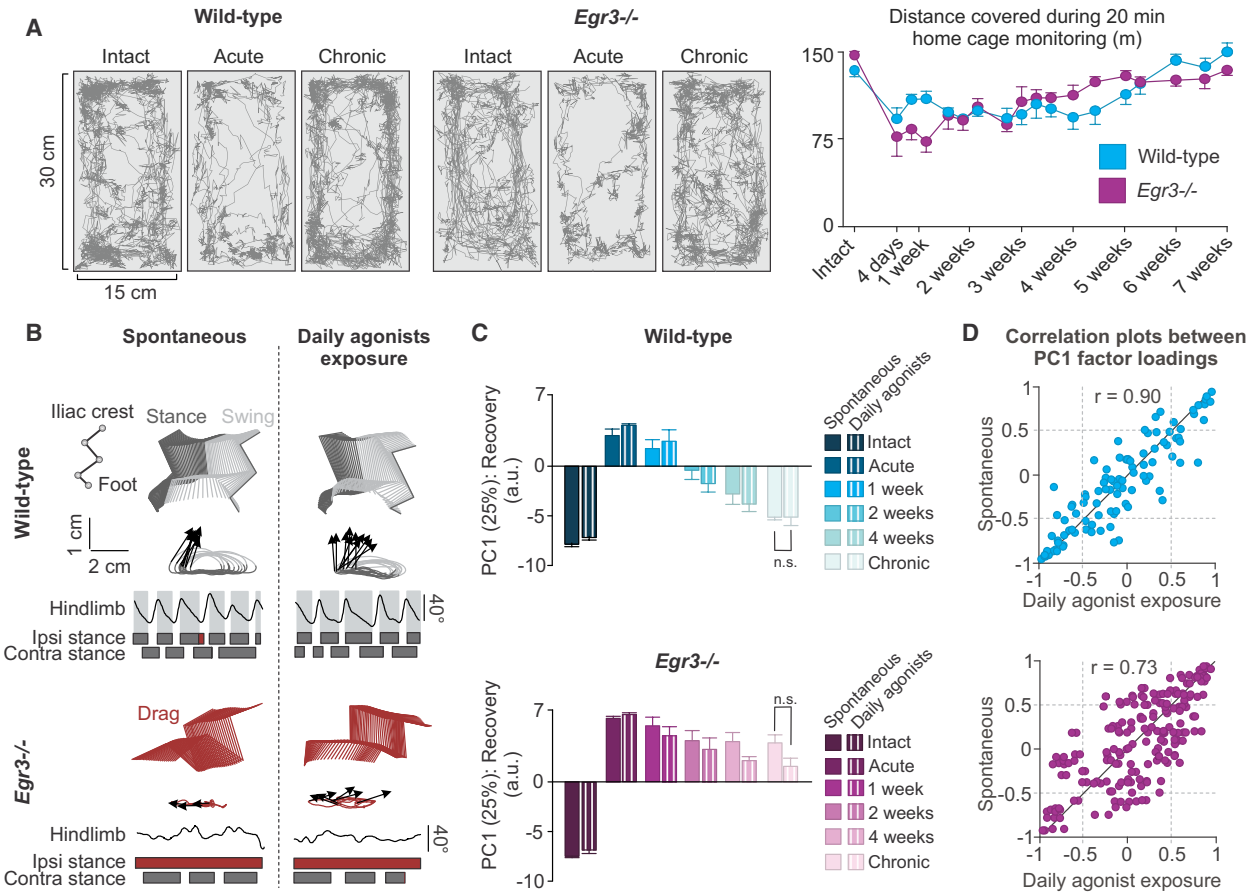

Figure 4. Impact of Activity on Functional Recovery after Spinal Cord Injury

(A) Body trajectories measured during the first 5 min of home cage monitoring for wild-type (n = 4) and *Egr3* mutant (n = 3) mice. Quantification of distance covered during 20 min period at intact condition and throughout recovery (p = 0.86; no significant effect of genotype).

(B) Stick representation of hindlimb movement at the chronic stage during treadmill locomotion shown for spontaneous and daily agonist exposure groups (below: concurrent limb endpoint trajectories and velocity vector at swing onset, together with ipsilesional hindlimb oscillations; dark gray bars, stance; red bars, dragging).

(C) Histogram plots reporting mean values of scores on recovery-related PC1 (25% explained variance) performed on ipsilesional gait patterns (average of 10–20 gait cycles/mouse, 108 parameters per gait cycle; n = 4 [agonist exposure] or 9 [spontaneous] wild-type and n = 5 [both conditions] *Egr3* mutant mice). Within genotype, scores are not different between spontaneous and daily agonist exposure groups before injury and throughout recovery process.

(D) Factor loadings (correlation of kinematic parameter and recovery-associated PC) of PC1 for all parameters (individual dots) of the two conditions (spontaneous recovery, daily agonist exposure) were correlated against each other for wild-type and *Egr3* mutant mice. Strong positive correlation represents similar recovery process in both spontaneous and agonist exposure groups for both genotypes.

Error bars, SEM; ns, not significant; acute, 3 days postinjury; chronic, 7 weeks postinjury. See also Figures S1 and S2.

gigantocellular, spinal vestibular, and red nucleus, as well as in M1 motor cortex (Figures 5B, 5C, and S5B). These findings reveal an absence of significant baseline differences between wild-type and *Egr3* mutant mice, allowing direct comparison of descending projection neuron populations across genotypes after injury.

At the acute stage, the majority of ipsilesional brainstem nuclei were not labeled. This depletion results from the disrupted access of ipsilaterally projecting brainstem nuclei to circuits below lesion. Lesion also disconnected contralaterally projecting descending pathways that decussate above lesion, e.g., leading to a lack of Rab-FP^{ON} neurons in M1 motor cortex and the red nucleus (Figures 5B, 5C, and S5B). In contrast, we detected a fraction of retrogradely marked spinal vestibular neurons residing in the ipsilesional brainstem (Figures 5B, 5C, and S5B). Axons of such neurons cross the midline above lesion, descend the spinal cord contralaterally, and establish collaterals crossing the midline a second time below lesion. We classified neurons with such axonal trajectories as dual midline-crossing projection neurons.

At chronic stages, we detected substantial reorganization of ipsilesional brainstem pathways in wild-type mice. Magnocellular, gigantocellular, and pontine nuclei contained significantly more ipsilesional Rab-FP^{ON} neurons than at acute stages (Figures 5B, 5C, and S5B). The presence of retrogradely labeled neurons in the ipsilesional brainstem thus implies that their axons

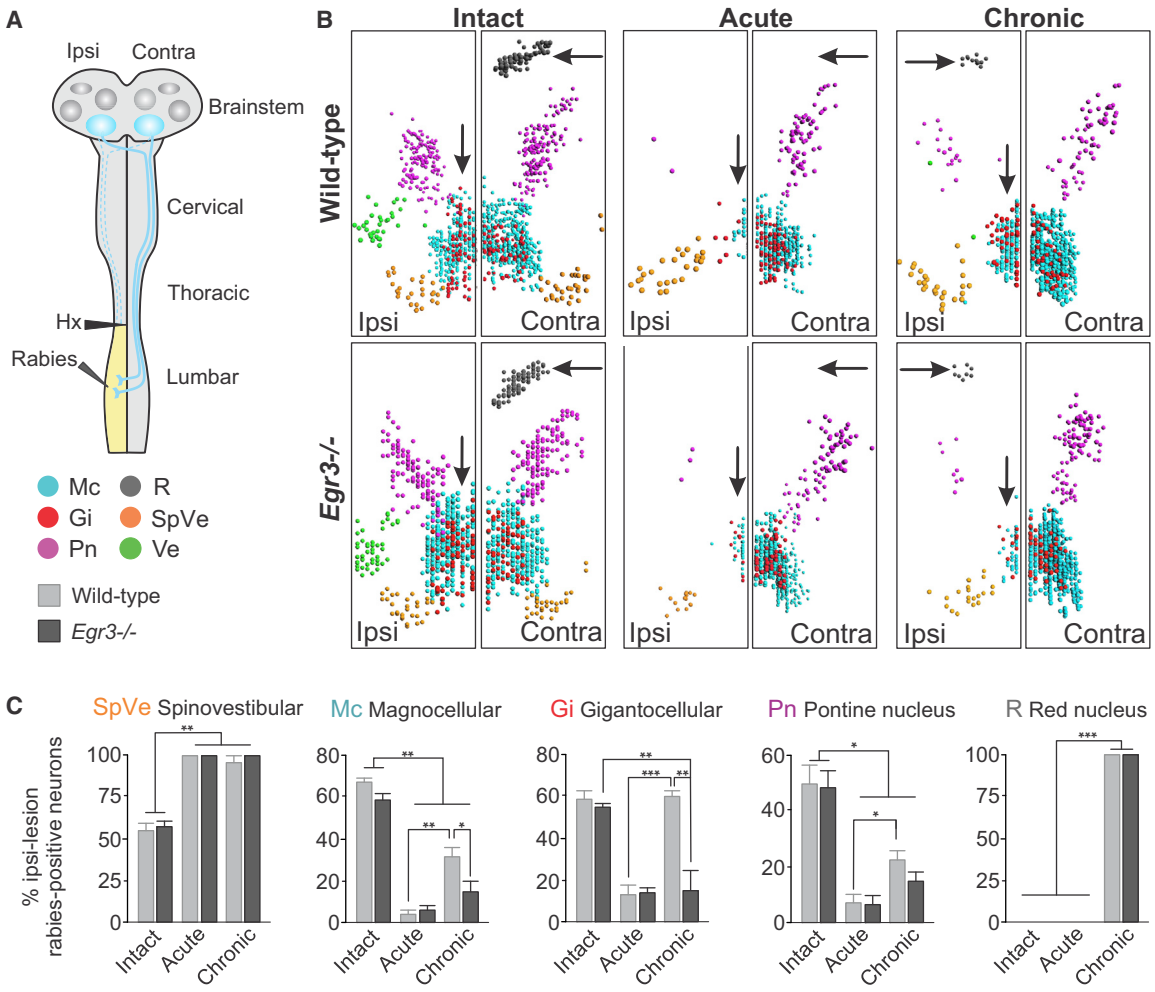

Figure 5. Reduced Injury Responses in Brainstem Pathways of *Egr3* Mutant Mice

(A) Diagram illustrating rabies virus injection strategy to retrogradely label brainstem neurons with descending projections to ipsilesional lumbar spinal cord (yellow). Bottom: display of different brainstem nuclei (Esposito et al., 2014; Paxinos and Franklin, 2012): Mc, magnocellular nucleus; Gi, Gigantocellular nucleus; Pn, Pontine nucleus; R, red nucleus; SpVe, spinal vestibular nucleus; Ve, vestibular nucleus.

(B) Top-down snapshots of 3D brainstem reconstructions in wild-type (top) and *Egr3* mutant (bottom) mice at intact, acute, and chronic stages (ipsi- and contralesional halves of the reconstruction displayed separately; each neuron represented by single dot; for color-code, see A).

(C) Quantification of brainstem reconstruction data (n = 3 each for intact and acute wild-type and *Egr3* mutant, n = 4 each for chronic wild-type and *Egr3* mutant) displaying percentage of ipsilesional neurons of entire rabies-marked respective subpopulation.

*p < 0.05; **p < 0.01; ***p < 0.001; error bars, SEM; acute, 3 days postinjury; chronic, 7 weeks postinjury; Hx, hemisection. See also Figure S5.

cross the midline twice to establish novel dual midline-crossing pathways. In contrast, *Egr3* mutant mice showed reduced levels of brainstem projection reorganization, with no significant differences in ipsilesional Rab-FP^{ON} neurons in magnocellular, gigantocellular, and pontine nuclei at chronic compared to acute stages (Figures 5B, 5C, and S5B). In contrast, we did not detect significant differences for neurons in the red nucleus between wild-type and *Egr3* mutant mice. Together, these results suggest that functional muscle spindle feedback facilitates rearrangement of specific descending pathways from the brainstem, but interestingly, not all populations were affected equally.

Next, we evaluated the effect of hemisection lesion on spinal projection neurons. We used rabies viruses to label neurons through their axonal projections (Figures S6A–S6C). We also exploited a transsynaptic virus-based approach with monosynaptic restriction to capture synaptic connectivity (Wickersham et al., 2007) (Figure 6). Both approaches revealed similar distribution patterns of spinal projection neurons across multiple segments of the spinal cord at intact stages in both wild-type and *Egr3* mutant mice (Figures 6 and S6A–S6C). At acute stages, only few ipsilesional spinal projection neurons exhibited dual midline-crossing circuitry (Figures 6B and 6C; Figures S6B and S6C). In contrast, contralesional spinal neurons were abundantly marked by Rab-FP. At chronic stages, Rab-FP injections in wild-type mice revealed a prominent increase in the percentage of ipsilesional neurons compared to acute stages (Figures 6B and

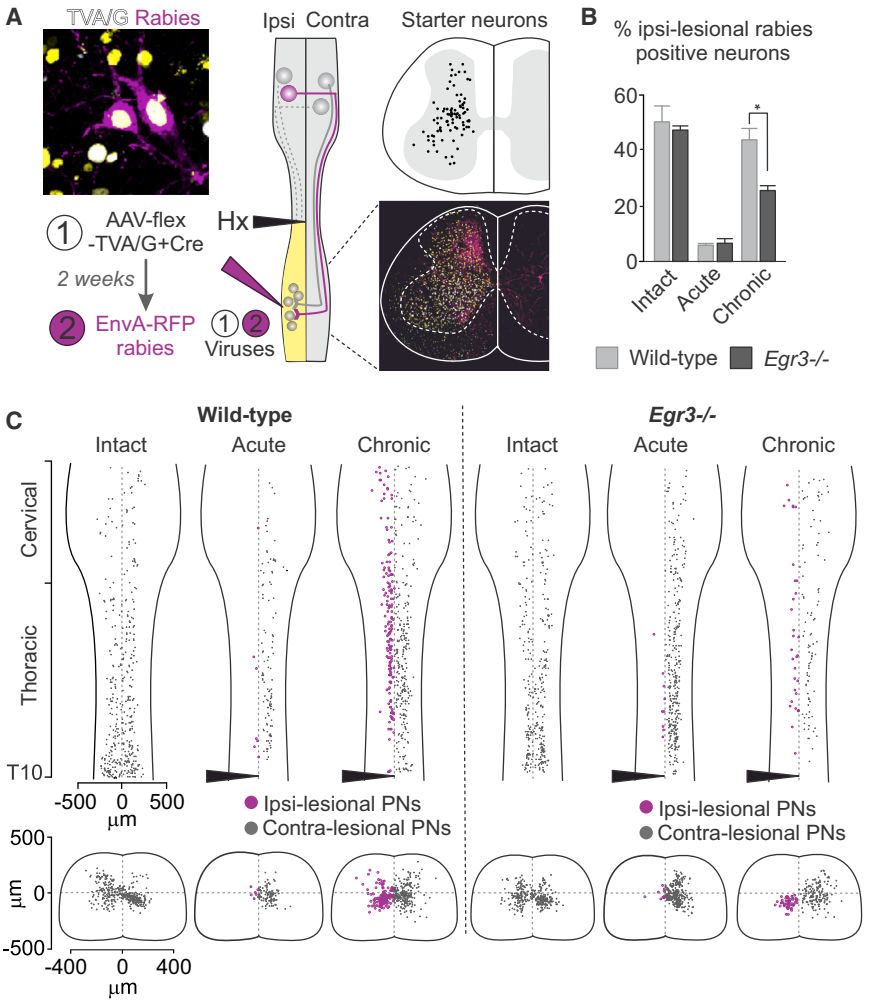

Figure 6. Detour Circuit Formation after Spinal Cord Injury Is Reduced in *Egr3* Mutant Mice

(A) Diagram illustrating monosynaptic rabies virus injection strategy to retrogradely mark descending spinal projection neurons with synaptic connections to ipsilesional neurons below lesion (injection at L2–L5; yellow; neurons with dotted axons, severed by injury; magenta, dual-crossing ipsilesional neurons). Top-left corner: example of triple-labeled (TVA/G/Rabies) neurons. Right: low-resolution view and reconstruction of triple-positive starter neurons of representative spinal cord section.

(B) Quantification of percentage of ipsilesional rabies positive spinal projection neurons above lesion with connections to ipsilesional starter neurons (n = 3 each for intact and acute wild-type and *Egr3* mutant; n = 4 for chronic wild-type; n = 5 for *Egr3* mutant).

(C) 3D reconstructions of supralesional spinal projection neurons with connection to ipsilesional lumbar circuits below lesion (yellow) in wild-type (left) and *Egr3* mutant (right) mice at intact, acute, and chronic stages in top-down longitudinal view (top) and transverse section (below) view (filled triangle, lesion position; gray line, midline; magenta, ipsilesional neurons).

*$p < 0.05$; error bars, SEM; acute, 3 days postinjury; chronic, 7 weeks postinjury; Hx, hemisection. See also Figure S6.

6C; Figures S6B and S6C). In *Egr3* mutant mice, however, their percentage above lesion was significantly lower than in wild-type mice (Figures 6B and 6C; Figures S6B and S6C). In contrast, we did not detect distribution differences of spinal projection neurons between genotypes below lesion (Figures S6D and S6E). Together, these results demonstrate that *Egr3* mutant mice exhibit a deficiency in the establishment of dual-crossing detour circuits involving multiple populations of descending projection neurons, whereas these are abundantly detected in wild-type mice.

Spinal Projection Neurons Connect to Deprived Circuits by Distinct Mechanisms

To gain insight into the cellular mechanisms responsible for the emergence of ipsilesional dual-crossing detour circuits after hemisection, we devised anterograde virus-mediated tracing experiments from supralesional spinal segments. We used injections of viruses that allow visualizing axons and synapses of specific subpopulations of descending projection neurons. This strategy also enabled evaluation of circuit reorganization from contralesional neurons that are less amenable to assess with retrograde tracing approaches due to partial persistence of projections to ipsilesional circuits after lesion.

We conducted a series of anterograde tracing experiments from ipsilesional or contralesional circuits above injury (Figure 7A) by unilateral coinjections of AAV-Tomato and AAV-SynGFP or AAV-SynMyc to anterogradely track axonal trajectories and synaptic arborizations (Figures 7 and S7). In intact mice of both genotypes, cervical (C5–7) and thoracic (T7–8) neurons projected to lumbar levels bilaterally (Figure S7A). After injury, ipsilesional injections target commissural neurons with axonal tracts descending contralateral to cell body position, whereas contralesional injections target ipsilateral projection neurons with axonal tracts ipsilateral to cell body position (Figure 7A).

We found that for both ipsi- and contralesional injections, descending axon tracts were present bilaterally in the white matter above lesion (Figure S7B). After hemisection, tracts only persisted on the contralesional side below lesion, demonstrating that axon collaterals at lumbar levels were exclusively derived from neurons projecting through contralesional tracts (Figures 7A and S7B). Next, we determined the frequency of midline-crossing axon collaterals below lesion at 2 weeks postlesion, the earliest possible tracing time point, and at chronic stages (Figures 7B and 7C). At 2 weeks postinjury, no difference was observed for ipsi- or contralesional populations and their midline-crossing frequency between wild-type and *Egr3* mutant mice (Figure 7C). At chronic stages, *Egr3* mutants exhibited a significantly reduced number of midline-crossing axons derived from ipsilesional populations compared to wild-type

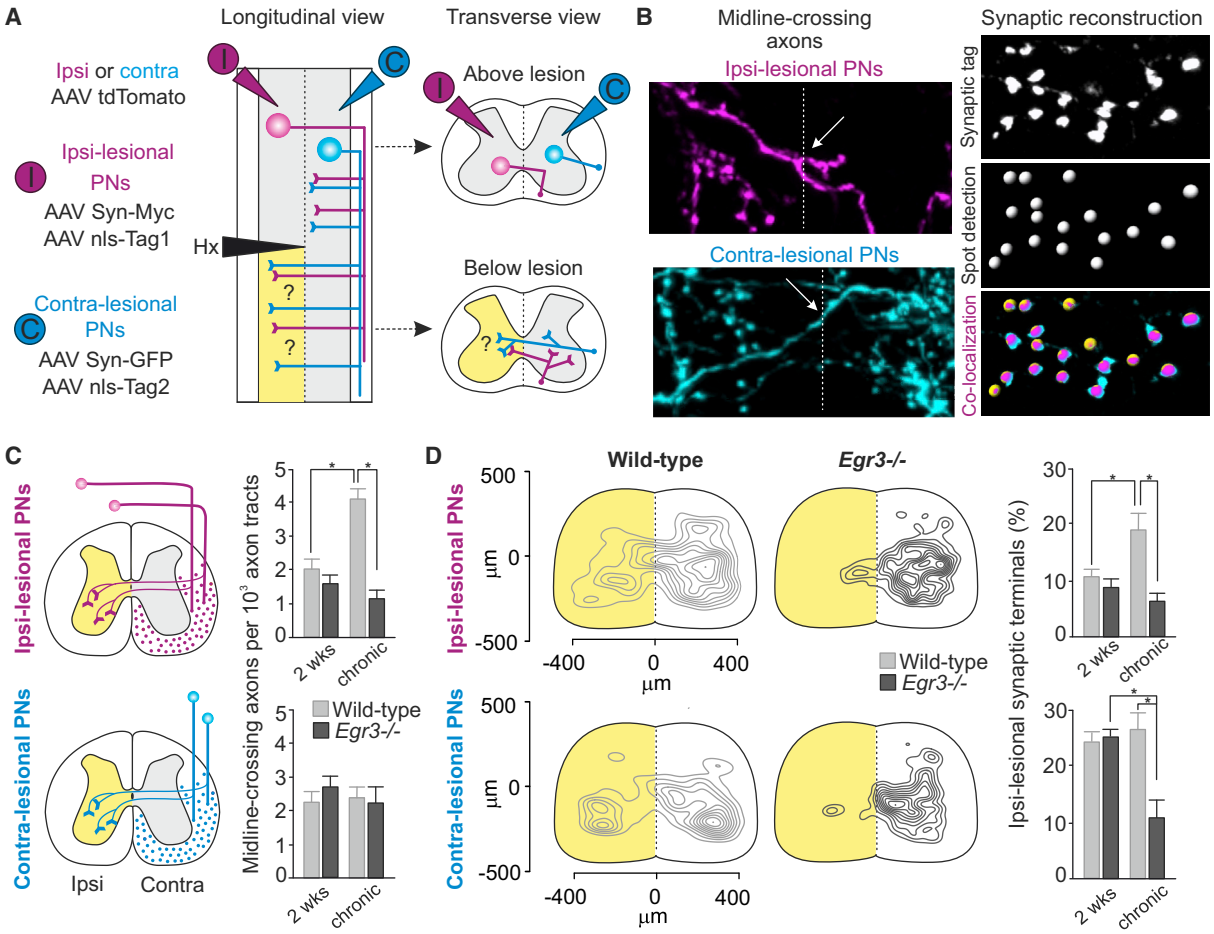

Figure 7. Distinct Reconnection Mechanisms for Spinal Projection Neuron Subpopulations

(A) Diagrams illustrating intraspinal injection scheme to anterogradely visualize axons (tdTomato) and synapses (synaptically tagged proteins) of ipsilesional (magenta) or contralesional (blue) spinal projection neuron residing above lesion (nuclear markers confirm unilaterality of injection). Top-down longitudinal and cross-section projected views shown (yellow, ipsilesional territory below lesion).

(B) Examples of midline-crossing axons and synaptic terminal analysis with high-resolution imaging and Imaris spot detection.

(C) Frequency analysis of midline-crossing axons originating from ipsi- and contralesional cervical spinal projection neurons, normalized to number of marked axons in contralesional white matter tracts below lesion (ipsilesion: n = 3 each for wild-type and *Egr3* mutant for both time points; contralesion: n = 4 for wild-type and n = 3 *Egr3* mutant for 2 week time point; n = 4 for wild-type and n = 5 *Egr3* mutant for chronic analysis).

(D) Quantitative analysis of distribution and density of synaptic terminals in the spinal cord below injury, originating from ipsi- and contralesional cervical spinal projection neurons (yellow, ipsilesional territory below lesion; ipsilesion, n = 4 for wild-type and n = 5 for *Egr3* mutant for 2 week time point; n = 5 for wild-type and n = 6 for *Egr3* mutant for chronic analysis; contra-lesion, n = 4 for wild-type and n = 6 for *Egr3* mutant for 2 week time point; n = 5 each for wild-type and *Egr3* mutant for chronic analysis). Contour plots show overall distribution of terminals from one chronic animal for each genotype; histogram plots display percentage of ipsilesional synaptic terminals at analyzed segmental spinal levels.

*p < 0.05; error bars, SEM; Hx, hemisection; PN, projection neuron; chronic, 7 weeks postinjury. See also Figure S7.

mice, whereas no significant difference was observed for contralesional populations (Figures 7C and S7F). Together, these findings indicate that the absence of muscle spindle feedback impairs the ability to establish de novo dual midline-crossing axons originating from ipsilesional spinal projection neurons and that these anatomical differences between the two genotypes become apparent later than 2 weeks after injury.

Next, we quantified ipsilesional synaptic arborization of midline-crossing axons (Figures 7B and 7D; Figures S7D and S7G). We reconstructed synaptic puncta at high resolution, yielding quantitative information on the spatial distribution and number of synaptic terminals (Figure 7B). Analysis of ipsi- and contralesional projection neurons revealed comparable synaptic innervation above lesion between wild-type and *Egr3* mutant mice (Figure S7D). In wild-type mice at chronic stages below lesion, synaptic input to ipsilesional gray matter targeted the ventrolateral quadrant, which contains many locomotor interneurons and motor neurons (Figures 7D and S7G). In contrast, the distribution of synaptic input beyond the midline in *Egr3* mutant mice was primarily confined to medially located territory (Figures 7D and S7G). The observed increase in synaptic terminals in wild-type mice was not present 2 weeks postlesion,

in agreement with the corresponding time course of midline-crossing axon elaboration (Figures 7C and 7D). For contralesional projection neurons, we also detected lower synaptic terminal density in the ipsilesional gray matter below lesion in *Egr3* mutant mice at chronic stages compared to wild-type mice, despite a similar number of midline-crossing axons in both genotypes (Figures 7C and 7D; Figures S7D and S7G). Strikingly, however, we found a selective decrease in the density of synaptic terminals between 2 weeks postlesion and chronic stages in *Egr3* mutant mice, ultimately leading to the observed lower terminal density compared to wild-type mice (Figure 7D). Together, our findings provide evidence that after lateral hemisection spinal cord injury, muscle spindle feedback enhances the process of axonal and synaptic rearrangements of multiple descending spinal projection neuron populations through distinct mechanisms.

DISCUSSION

Spinal cord injuries lead to immediate motor dysfunction because of separation of descending control pathways from local spinal circuits. Various degrees of functional recovery occur after incomplete injury. However, the likely involvement of numerous circuit elements paired with the limited understanding of their precise organization and function within the hierarchy of motor control pathways have posed challenges for gaining mechanistic insight in the process of functional recovery. Here, we demonstrate that muscle spindle feedback circuits are essential to direct locomotor recovery after lateral hemisection spinal cord injury and that the lack of this specific sensory channel affects the ability of descending projection neurons to undergo efficient circuit reorganization after injury. We discuss our findings with an emphasis on the role of sensory feedback circuits in locomotor improvement after injury and the mechanisms by which circuit rearrangements parallel and influence the recovery process.

Task-Specific Locomotor Recovery after Spinal Cord Injury in Wild-Type Mice

Wild-type mice improve basic locomotor function after hemisection spinal cord injury to a significant extent. In contrast, they remain severely compromised in their ability to carry out precision ladder walking. These findings underscore the need for task-specific communication channels between supraspinal and spinal circuits, some of which do not recover after injury. A possible model to explain these findings is that upon establishment of multistep synaptic relays, a comparatively crude wiring of descending circuit elements is sufficient to drive disconnected ipsilesional spinal circuits below lesion for regaining basic locomotor function. Newly established descending connections can interact with an already wired repertoire of local spinal circuits able to coordinate basic locomotor behaviors. In contrast, precision tasks likely require specific and refined descending circuit connectivity. In addition, complex tasks may depend more heavily on information conveyed through ascending pathways, which exhibit enduring dysfunction after spinal cord injury (Kaas et al., 2008; Martinez et al., 2010). Taken together, these observations suggest that distinct neuronal circuit elements are responsible and necessary for the re-establishment of task-specific functions.

Role of Muscle Spindle Feedback Circuits in Locomotor Recovery after Spinal Cord Injury

Muscle spindle afferents constitute a minor fraction of DRG sensory neurons (Scott, 1992), but our results demonstrate that they are essential to promote locomotor recovery after incomplete spinal cord lesion. Why does deprivation of a specific sensory channel lead to such profound impairment? Each class of functionally distinct sensory neurons exhibits lamina-specific axonal terminations in the spinal cord (Brown, 1981). While cutaneous and mechanoreceptive afferents target dorsal horn neurons, proprioceptive afferents terminate more ventrally, raising the possibility that these differential synaptic connectivity profiles may contribute to their role in the recovery process.

A primary mode of action by muscle spindle afferents in facilitating recovery may involve recruitment of motor circuits through their unique connections. Targeted circuit elements include motor neurons and core components of ventral locomotor interneuron circuits that have recently been demonstrated to play important roles in the regulation of extensor-flexor alternation (Talpalar et al., 2011; Zhang et al., 2014) and rhythm generation (Dougherty et al., 2013) in the mouse. The pivotal role of muscle spindle feedback in promoting locomotor improvement after lateral hemisection observed here might therefore be at least in part attributed to their direct synaptic access to these neurons. Specifically, muscle spindle afferents are embedded in a highly selective central synaptic connectivity matrix. Transfer of muscle-specific information to functionally distinct interneurons that directly activate motor neurons or mediate reciprocal inhibition between motor neurons is a key feature of these neuronal networks (Jankowska and Edgley, 1993; McCrea and Rybak, 2008; Pearson, 2008; Wang et al., 2008; Windhorst, 2007). Muscle spindle afferent recruitment after injury may strengthen these specific spinal circuits and their connections (Petruska et al., 2007), whereas their functional absence in *Egr3* mutants might contribute to the severe impairment in recovery.

An alternative or complementary possibility is that muscle spindle afferents release factors in an activity-dependent manner, which in turn promote circuit reorganization in the spinal cord. For instance, retrograde trophic support by the neurotrophin NT-3 strengthens synaptic connections (Boyce and Mendell, 2014; Chen et al., 2002; Oakley et al., 1997). Moreover, the amount of physical activity influences baseline BDNF expression in the spinal cord after traumatic injury (Ying et al., 2008), an effect that may be mediated by recruitment of muscle spindle feedback circuits. In our experiments, we found no difference in the degree of spontaneous cage activity between wild-type and *Egr3* mutants after hemisection spinal cord injury, excluding disparity in physical activity as a possible reason for differential recovery. In addition, daily application of monoaminergic agents to enhance activity of local spinal circuits in an attempt to bypass reduced sensory feedback in *Egr3* mutant mice was inefficient in overcoming the severely limited recovery in *Egr3* mutant mice. These findings demonstrate that muscle spindle afferents, despite being a numerically minor sensory

neuron population, play an instrumental and selective role in promoting functional recovery after spinal cord injury.

Formation of Spinal Detour Circuits Parallels Locomotor Recovery

Regaining locomotor function of the ipsilesional hindlimb after thoracic hemisection requires the establishment of detour circuits that reconnect descending pathways to deprived locomotor circuits below lesion. The formation of such detour circuits to functionally bridge the injury site depends on local axon growth and reorganization of synaptic connectivity within existing descending circuit modules (Ballermann and Fouad, 2006; Bareyre et al., 2004; Courtine et al., 2008; Jankowska and Edgley, 2006; Rosenzweig et al., 2010; van den Brand et al., 2012). We demonstrate that in wild-type mice, injury-induced circuit-level responses involve the deployment of specific patterns of axonal growth and synaptic arborization from distinct populations of supraspinal and spinal projection neurons.

Our anatomical mapping to identify injury-responsive descending circuit elements above lesion demonstrates that reduced compensatory responses to injury are widespread in *Egr3* mutants. These alterations include ipsi- and contralesional spinal projection neurons at multiple spinal segments and specific descending pathways from the brainstem. Perturbation or silencing of any identified specific neuron population alone in wild-type mice is therefore unlikely to recapitulate the dramatic lack of recovery observed in *Egr3* mutant mice. On the other hand, experimental attempts to specifically target a majority of neurons undergoing novel collateral formation after injury would require injections at multiple central nervous system (CNS) sites, likely themselves inducing behavioral repercussions. In addition, even if successful, such approaches would interfere with the function of targeted neurons in their entirety, and not just with the newly formed collaterals.

How does muscle spindle feedback facilitate de novo circuit formation? While we cannot rule out multifaceted circuit-level effects influencing the recovery process, we favor a model in which muscle spindle feedback circuits act primarily on ipsilesional circuits below the injury site to promote the formation of compensatory connections to deprived circuits. In agreement with such a model, identified brainstem populations do not receive direct synaptic input from muscle spindle afferents, implying that at least for these populations such input is not essential to trigger circuit reorganization. Mechanistically, the assembly of novel circuits in the adult nervous system may be achieved through stabilization of nascent axon collaterals involving Hebbian plasticity reinforced by muscle spindle afferent input. Growth and stabilization of axons in the developing nervous system suggests that such mechanisms act in highly cell-type-specific patterns (Andreae and Burrone, 2014).

To gain insight into how defined neuronal populations respond to injury, we focused our anterograde synaptic mapping analysis on spinal projections neurons. Comparison of wild-type and *Egr3* mutant mice uncovered distinct responses for specific spinal populations. Ipsilesional descending spinal projection neurons in *Egr3* mutants exhibited both a reduction in dual midline-crossing axons and decreased ipsilesional synaptic arborization below lesion, occurring later than 2 weeks after injury. In contrast, contralesional counterparts only showed restricted arborization of synaptic terminals without disruption in midline-crossing axons. These synaptic differences however can be attributed to synaptic pruning in the absence of muscle spindle feedback rather than additional synaptic growth in wild-type mice. These findings also suggest that the majority of injury-responsive contralesional spinal projection neurons already possess midline-crossing collaterals at intact stages, providing an explanation for why this parameter is not affected in *Egr3* mutants compared to wild-type mice at chronic stages.

In summary, our study demonstrates that one specific sensory channel has an executive role in directing restoration of hindlimb motor function and facilitating multifaceted circuit reorganization after incomplete spinal cord injury. These findings stress the importance of exploiting muscle spindle feedback circuits in the design of rehabilitative strategies after spinal cord injury. Epidural stimulation of lumbar segments facilitates motor control and leads to improved functional recovery in animal models and paraplegic individuals (Angeli et al., 2014; van den Brand et al., 2012). This treatment paradigm may at least in part act through the recruitment of myelinated sensory feedback circuits (Capogrosso et al., 2013). Refined experimental strategies to specifically modulate muscle spindle feedback channels open innovative therapeutic avenues to pursue in the future. Similar concepts may apply to other traumatic CNS disorders, such as stroke or brain injury, which heavily rely on plasticity of both supraspinal and spinal descending pathways to regain functional capacities after lesion.

EXPERIMENTAL PROCEDURES

Mouse Genetics and Surgeries

Mice used were from a local colony containing the *Egr3* mutant allele previously described (Tourtellotte and Milbrandt, 1998). Surgical procedures for hemisection injury and EMG implantation have been described previously (Courtine et al., 2008) and were performed under full general anesthesia with isoflurane in oxygen-enriched air (1%–2%). Local Swiss veterinary offices approved all the procedures. Details on mice and surgical procedures are described in the Extended Experimental Procedures.

Behavioral Analysis

Whole-body kinematics were recorded using the high-speed motion capture system Vicon (Vicon Motion Systems), combining 10–12 infrared cameras (200 Hz) (van den Brand et al., 2012). Parameters describing kinematic and EMG characteristics were computed using custom-written MATLAB scripts (van den Brand et al., 2012). Behavioral tests included overground locomotion on an elevated runway, stepping on a motorized treadmill (Robomedica), elevated horizontal ladder, and swimming. To quantify task- and genotype-specific gait characteristics prior to injury and throughout the recovery process after hemisection spinal cord injury, we implemented a multistep statistical procedure based on PC analysis (Dominici et al., 2012). A flowchart explaining the various steps of this analysis can be found in Figure S2. For behavioral monitoring of home cage activity, spontaneous activity was surveyed for each mouse during 20 min. Additional information on recordings, postprocessing and behavioral tasks are available in the Extended Experimental Procedures and Figure S2.

Anatomical Tracing Experiments

Rabies viruses and AAVs were amplified and purified from local viral stocks following established protocols (Esposito et al., 2014; Pivetta et al., 2014; Wickersham et al., 2010). Additional information on production and injection

of viruses, antibodies, imaging, and anatomical quantification can be found in the Extended Experimental Procedures.

Statistical Analysis

All data are reported as mean values ± SEM. All statistical evaluations were performed using GraphPad Prism (v. 6.0) (Prism, GraphPad Software) using unpaired Student's t test (Figures 1C, 1D, 2D, 5C, 6B, 7C, and 7D; Figures S3A, S3B, S4D, S6C, S7A, S7B, S7D, S7F, and S7G), two-way ANOVA for repeated measurement (Figures 1D, 3D, 3E, 4A, and 4C; Figures S3D, S3E, S5A, and S5B), and one-way ANOVA for repeated measurements (Figure S5C), followed by post hoc comparisons (Šídák-Bonferroni). The significance level for behavioral analysis was set as $|R \text{ value}| > 0.5$ and $p < 0.05$, respectively. Significance level is defined as follows for all analyses performed: $^{*}p < 0.05$; $^{**}p < 0.01$; $^{***}p < 0.001$.

SUPPLEMENTAL INFORMATION

Supplemental Information includes Extended Experimental Procedures, seven figures, and five movies and can be found with this article online at http://dx.doi.org/10.1016/j.cell.2014.11.019.

AUTHOR CONTRIBUTIONS

A.T., G.C., and S.A. initiated the project. A.T. and I.V. performed behavioral experiments and analysis; A.T. performed anatomy experiments and analysis. All authors were involved in interpretation of experiments and contributed to writing the paper.

ACKNOWLEDGMENTS

We are grateful to M. Sigrist, M. Mielich, P. Capelli, and S. Esposito for expert technical help, M. Kirschmann, S. Bourke, and L. Gelman from the FMI imaging facility, N. Ehrenfurchter from the Biozentrum Imaging facility for help and advice with image acquisition and analysis, and P. Caroni for discussions and comments on the manuscript. A.T. and S.A. were supported by an ERC Advanced Grant, the Swiss National Science Foundation, the Kanton Basel-Stadt, and the Novartis Research Foundation. I.V. was supported by the European Neuroscience Campus (ENC) network. G.C. was supported by an ERC Starting Grant and the International Foundation for Research in Paraplegia (IRP).

Received: August 13, 2014
Revised: November 5, 2014
Accepted: November 11, 2014
Published: December 18, 2014

REFERENCES

Andreae, L.C., and Burrone, J. (2014). The role of neuronal activity and transmitter release on synapse formation. Curr. Opin. Neurobiol. *27*, 47–52.

Angeli, C.A., Edgerton, V.R., Gerasimenko, Y.P., and Harkema, S.J. (2014). Altering spinal cord excitability enables voluntary movements after chronic complete paralysis in humans. Brain *137*, 1394–1409.

Arshavskiĭ, Iul., Kots, IaM., Orlovskiĭ, G.N., Rodionov, I.M., and Shik, M.L. (1965). [Study of biomechanics of running dogs]. Biofizika *10*, 665–671.

Ballermann, M., and Fouad, K. (2006). Spontaneous locomotor recovery in spinal cord injured rats is accompanied by anatomical plasticity of reticulospinal fibers. Eur. J. Neurosci. *23*, 1988–1996.

Bareyre, F.M., Kerschensteiner, M., Raineteau, O., Mettenleiter, T.C., Weinmann, O., and Schwab, M.E. (2004). The injured spinal cord spontaneously forms a new intraspinal circuit in adult rats. Nat. Neurosci. *7*, 269–277.

Bouyer, L.J., and Rossignol, S. (2003). Contribution of cutaneous inputs from the hindpaw to the control of locomotion. II. Spinal cats. J. Neurophysiol. *90*, 3640–3653.

Boyce, V.S., and Mendell, L.M. (2014). Neurotrophins and spinal circuit function. Front. Neural Circuits *8*, 59.

Brown, A.G. (1981). Organization of the Spinal Cord (New York: Springer Verlag).

Capogrosso, M., Wenger, N., Raspopovic, S., Musienko, P., Beauparlant, J., Bassi Luciani, L., Courtine, G., and Micera, S. (2013). A computational model for epidural electrical stimulation of spinal sensorimotor circuits. J. Neurosci. *33*, 19326–19340.

Chen, H.H., Tourtellotte, W.G., and Frank, E. (2002). Muscle spindle-derived neurotrophin 3 regulates synaptic connectivity between muscle sensory and motor neurons. J. Neurosci. *22*, 3512–3519.

Courtine, G., Song, B., Roy, R.R., Zhong, H., Herrmann, J.E., Ao, Y., Qi, J., Edgerton, V.R., and Sofroniew, M.V. (2008). Recovery of supraspinal control of stepping via indirect propriospinal relay connections after spinal cord injury. Nat. Med. *14*, 69–74.

Curt, A., Van Hedel, H.J., Klaus, D., and Dietz, V.; EM-SCI Study Group (2008). Recovery from a spinal cord injury: significance of compensation, neural plasticity, and repair. J. Neurotrauma *25*, 677–685.

Dietz, V., and Fouad, K. (2014). Restoration of sensorimotor functions after spinal cord injury. Brain *137*, 654–667.

Dougherty, K.J., Zagoraiou, L., Satoh, D., Rozani, I., Doobar, S., Arber, S., Jessell, T.M., and Kiehn, O. (2013). Locomotor rhythm generation linked to the output of spinal shox2 excitatory interneurons. Neuron *80*, 920–933.

Eccles, J.C., Eccles, R.M., and Lundberg, A. (1957). The convergence of monosynaptic excitatory afferents on to many different species of alpha motoneurones. J. Physiol. *137*, 22–50.

Edgerton, V.R., Courtine, G., Gerasimenko, Y.P., Lavrov, I., Ichiyama, R.M., Fong, A.J., Cai, L.L., Otoshi, C.K., Tillakaratne, N.J., Burdick, J.W., and Roy, R.R. (2008). Training locomotor networks. Brain Res. Brain Res. Rev. *57*, 241–254.

Esposito, M.S., Capelli, P., and Arber, S. (2014). Brainstem nucleus MdV mediates skilled forelimb motor tasks. Nature *508*, 351–356.

Gruner, J.A., and Altman, J. (1980). Swimming in the rat: analysis of locomotor performance in comparison to stepping. Exp. Brain Res. *40*, 374–382.

Halbertsma, J.M. (1983). The stride cycle of the cat: the modelling of locomotion by computerized analysis of automatic recordings. Acta Physiol. Scand. Suppl. *521*, 1–75.

Jankowska, E., and Edgley, S. (1993). Interactions between pathways controlling posture and gait at the level of spinal interneurones in the cat. Prog. Brain Res. *97*, 161–171.

Jankowska, E., and Edgley, S.A. (2006). How can corticospinal tract neurons contribute to ipsilateral movements? A question with implications for recovery of motor functions. Neuroscientist *12*, 67–79.

Kaas, J.H., Qi, H.X., Burish, M.J., Gharbawie, O.A., Onifer, S.M., and Massey, J.M. (2008). Cortical and subcortical plasticity in the brains of humans, primates, and rats after damage to sensory afferents in the dorsal columns of the spinal cord. Exp. Neurol. *209*, 407–416.

Knikou, M., and Mummidisetty, C.K. (2014). Locomotor training improves premotoneuronal control after chronic spinal cord injury. J. Neurophysiol. *111*, 2264–2275.

Lavrov, I., Courtine, G., Dy, C.J., van den Brand, R., Fong, A.J., Gerasimenko, Y., Zhong, H., Roy, R.R., and Edgerton, V.R. (2008). Facilitation of stepping with epidural stimulation in spinal rats: role of sensory input. J. Neurosci. *28*, 7774–7780.

Maier, I.C., and Schwab, M.E. (2006). Sprouting, regeneration and circuit formation in the injured spinal cord: factors and activity. Philos. Trans. R. Soc. Lond. B Biol. Sci. *361*, 1611–1634.

Martinez, M., Delcour, M., Russier, M., Zennou-Azogui, Y., Xerri, C., Coq, J.O., and Brezun, J.M. (2010). Differential tactile and motor recovery and cortical map alteration after C4-C5 spinal hemisection. Exp. Neurol. *221*, 186–197.

McCrea, D.A., and Rybak, I.A. (2008). Organization of mammalian locomotor rhythm and pattern generation. Brain Res. Brain Res. Rev. *57*, 134–146.

Oakley, R.A., Lefcort, F.B., Clary, D.O., Reichardt, L.F., Prevette, D., Oppenheim, R.W., and Frank, E. (1997). Neurotrophin-3 promotes the differentiation

of muscle spindle afferents in the absence of peripheral targets. J. Neurosci. *17*, 4262–4274.

Paxinos, G., and Franklin, K.B. (2012). The Mouse Brain in Stereotaxic Coordinates, Fourth Edition (San Diego: Elsevier).

Pearson, K.G. (2008). Role of sensory feedback in the control of stance duration in walking cats. Brain Res. Brain Res. Rev. *57*, 222–227.

Petruska, J.C., Ichiyama, R.M., Jindrich, D.L., Crown, E.D., Tansey, K.E., Roy, R.R., Edgerton, V.R., and Mendell, L.M. (2007). Changes in motoneuron properties and synaptic inputs related to step training after spinal cord transection in rats. J. Neurosci. *27*, 4460–4471.

Pivetta, C., Esposito, M.S., Sigrist, M., and Arber, S. (2014). Motor-circuit communication matrix from spinal cord to brainstem neurons revealed by developmental origin. Cell *156*, 537–548.

Ramon y Cajal, S. (1928). Degeneration and Regeneration of the Nervous System (Oxford: Oxford University Press).

Rosenzweig, E.S., Courtine, G., Jindrich, D.L., Brock, J.H., Ferguson, A.R., Strand, S.C., Nout, Y.S., Roy, R.R., Miller, D.M., Beattie, M.S., et al. (2010). Extensive spontaneous plasticity of corticospinal projections after primate spinal cord injury. Nat. Neurosci. *13*, 1505–1510.

Rossignol, S., and Frigon, A. (2011). Recovery of locomotion after spinal cord injury: some facts and mechanisms. Annu. Rev. Neurosci. *34*, 413–440.

Rossignol, S., Dubuc, R., and Gossard, J.P. (2006). Dynamic sensorimotor interactions in locomotion. Physiol. Rev. *86*, 89–154.

Roy, R.R., Harkema, S.J., and Edgerton, V.R. (2012). Basic concepts of activity-based interventions for improved recovery of motor function after spinal cord injury. Arch. Phys. Med. Rehabil. *93*, 1487–1497.

Scott, S.A. (1992). Sensory Neurons: Diversity, Development and Plasticity (New York: Oxford University Press).

Talpalar, A.E., Endo, T., Löw, P., Borgius, L., Hägglund, M., Dougherty, K.J., Ryge, J., Hnasko, T.S., and Kiehn, O. (2011). Identification of minimal neuronal networks involved in flexor-extensor alternation in the mammalian spinal cord. Neuron *71*, 1071–1084.

Tello, F. (1907). La regeneration dans les voies optiques. Trab. Lab. Invest. Biol. Univ. Madr. *5*, 237–248.

Tourtellotte, W.G., and Milbrandt, J. (1998). Sensory ataxia and muscle spindle agenesis in mice lacking the transcription factor Egr3. Nat. Genet. *20*, 87–91.

van den Brand, R., Heutschi, J., Barraud, Q., DiGiovanna, J., Bartholdi, K., Huerlimann, M., Friedli, L., Vollenweider, I., Moraud, E.M., Duis, S., et al. (2012). Restoring voluntary control of locomotion after paralyzing spinal cord injury. Science *336*, 1182–1185.

Wang, Z., Li, L., Goulding, M., and Frank, E. (2008). Early postnatal development of reciprocal Ia inhibition in the murine spinal cord. J. Neurophysiol. *100*, 185–196.

Wickersham, I.R., Sullivan, H.A., and Seung, H.S. (2010). Production of glycoprotein-deleted rabies viruses for monosynaptic tracing and high-level gene expression in neurons. Nat. Protoc. *5*, 595–606.

Wickersham, I.R., Lyon, D.C., Barnard, R.J., Mori, T., Finke, S., Conzelmann, K.K., Young, J.A., and Callaway, E.M. (2007). Monosynaptic restriction of transsynaptic tracing from single, genetically targeted neurons. Neuron *53*, 639–647.

Windhorst, U. (2007). Muscle proprioceptive feedback and spinal networks. Brain Res. Bull. *73*, 155–202.

Ying, Z., Roy, R.R., Zhong, H., Zdunowski, S., Edgerton, V.R., and Gomez-Pinilla, F. (2008). BDNF-exercise interactions in the recovery of symmetrical stepping after a cervical hemisection in rats. Neuroscience *155*, 1070–1078.

Zhang, J., Lanuza, G.M., Britz, O., Wang, Z., Siembab, V.C., Zhang, Y., Velasquez, T., Alvarez, F.J., Frank, E., and Goulding, M. (2014). V1 and v2b interneurons secure the alternating flexor-extensor motor activity mice require for limbed locomotion. Neuron *82*, 138–150.

Zörner, B., Filli, L., Starkey, M.L., Gonzenbach, R., Kasper, H., Röthlisberger, M., Bolliger, M., and Schwab, M.E. (2010). Profiling locomotor recovery: comprehensive quantification of impairments after CNS damage in rodents. Nat. Methods *7*, 701–708.

Zörner, B., Bachmann, L.C., Filli, L., Kapitza, S., Gullo, M., Bolliger, M., Starkey, M.L., Röthlisberger, M., Gonzenbach, R.R., and Schwab, M.E. (2014). Chasing central nervous system plasticity: the brainstem's contribution to locomotor recovery in rats with spinal cord injury. Brain *137*, 1716–1732.